

Improved rate-based modeling of carbon dioxide absorption with aqueous monoethanolamine solution

Stefania MOIOLI¹, Laura A. PELLEGRINI (✉)¹, Simone GAMBA¹, Ben LI²

¹ Department of Chemistry, Materials and Chemical Engineering “G. Natta”, I-20133 Milano, Italy

² School of Chemical Engineering, University of Science and Technology, Anshan 114051, China

1 Introduction

Carbon dioxide is a powerful greenhouse gas, whose massive presence in the atmosphere is a cause of gradual global warming. Once emitted, CO₂ added to the atmosphere and oceans remains for thousands of years. Thus, climate changes forced by CO₂ depend primarily on cumulative emissions, making it more and more difficult to avoid further substantial effects on the environment. “Its concentration has increased every year since scientists started making measurements on the slopes of the Mauna Loa volcano more than five decades ago. The rate of increase has accelerated since the measurements started, from about 0.7 ppm per year in the late 1950s to 2.1 ppm per year during the last 10 years”, as stated by the National Oceanic and Atmospheric Administration (NOAA) [1]. On May 9th, 2013, the daily mean concentration of carbon dioxide in the atmosphere of Mauna Loa, Hawaii, was

400.03 parts per million (ppm), while on December 11th, 1997, the day the Kyoto Protocol was conceived [2], the CO₂ concentration was 364.40 ppm [1]. Thus, despite the efforts of many countries in reducing the CO₂ emissions in the atmosphere, its concentration has been still increasing. Lowering CO₂ emissions from anthropogenic activities plays an important role in addressing the global climate change.

Absorption by means of chemical solvents, such as monoethanolamine (MEA) is the most commonly used process for CO₂ removal. It can be applied to exhaust gases of power plants, natural gas, and refinery gas. Amine scrubbing involves several advantages, in particular the chemical reactions in the liquid phase enhance the mass transfer. The presence of the amine dramatically influences the solubility of the acid gas in water [3]. From the bulk of the gas phase to the bulk of the liquid phase, for what concerns the carbon dioxide absorption, the following steps occur: (i) diffusion of CO₂ from the bulk of the gas phase to the gas-liquid interface; (ii) reaction between dissolved CO₂ and liquid reactants (MEA and H₂O); (iii) diffusion of reaction products to the bulk of the liquid phase promoted by the concentration gradient due to chemical reaction.

This paper focuses on modeling and simulation of a post-combustion carbon dioxide capture in a coal-fired power plant by chemical absorption using MEA. Industrially, MEA is the most frequently used solvent for post-combustion acid gas removal [4] and the preferred solvent for CO₂ removal from gas streams at low CO₂ content, especially at low pressure. Among the advantages of MEA, its low molecular weight, resulting in high solution capacity at moderate concentrations (on a mass basis), and its high alkalinity can be cited [3]. Modeling the chemical absorption process requires the proper description of thermodynamics and mass transfer with kinetics [5,6]. These topics have been widely studied in literature. Kent and Eisenberg proposed the first approach to model

the amine treating process using an equilibrium model [7]. The rate-based approach, which is the most rigorous method to describe the mass transfer phenomenon, has become more applicable in the last years, since it is demanding in terms of computational time. Al-Baghli et al. [8] proposed a rate-based model based on film theory and on the assumption of thermodynamic equilibrium among the reacting species in the bulk. Similarly, using the two-film theory other researchers [9] studied the performance of an EU project pilot plant. The reaction kinetics was taken into account by Kucka et al. [10], who combined it with film theory in the computation of mass transfer. The eddy diffusivity theory, which allows the prediction of the correct dependence of the mass transfer coefficient on the diffusivity of carbon dioxide in the solvent, has been used [11]. In the paper presented by Freguia and Rochelle [11], an adjustment factor was used, in order to adjust the performance of the model. In this work, a mass transfer model based on the eddy diffusivity theory [12] is proposed and implemented in the ASPEN Plus[®] software [13], along with regressed parameters for the Electrolyte-NRTL model worked out in a previous research [14]. The mass transfer theory is used without resorting to any adjustable parameter, with the aim to obtain a reliable tool for process simulation, since the accuracy of the model is important for the design, performance and cost of MEA absorption [6].

2 Chemical reactions involving CO₂ and MEA

Because of chemical reactions, amines significantly affect the rate of absorption of acid gases in aqueous solutions. On a theoretical basis, a compound can reach a physical equilibrium between the vapor and the liquid phases. For example, gaseous CO₂ equilibrates with the molecular undissociated CO₂ in the aqueous phase. When carbon dioxide is absorbed in an aqueous solution containing an amine, it undergoes chemical reactions, so it is partially consumed and its bulk concentration becomes lower than in the case of physical absorption alone. Thus, the equilibrium solubility of an acid gas that reacts in the liquid phase is influenced both by the partial pressure of this gas over the liquid (as in the case of physical absorption) and by chemical reactions. As a consequence, the driving force for mass transfer, i.e. the difference between the gas concentration in the liquid at the gas-liquid interface and the unreacted gas concentration in the bulk of the liquid phase, is higher than that of the physical absorption process.

Since these reactions involve both molecular and ionic species, both equilibrium and kinetic controlled reactions should be taken into account to describe the process. Equilibrium reactions with a strongly temperature-dependent equilibrium constant are listed as follows:

(i) Dissociation of water [15]:



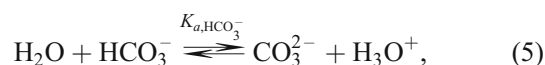
$$\ln K_{\text{H}_2\text{O}} = 132.89 - \frac{13446}{T} - 22.47 \ln T. \quad (2)$$

(ii) Hydrolysis of carbon dioxide [15]:



$$\ln K_{a,\text{CO}_2} = 231.46 - \frac{12092}{T} - 36.78 \ln T. \quad (4)$$

(iii) Dissociation of bicarbonate ion [15]:



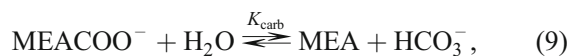
$$\ln K_{a,\text{HCO}_3^-} = 216.05 - \frac{12432}{T} - 35.48 \ln T. \quad (6)$$

(vi) Dissociation of protonated monoethanolamine [13]:



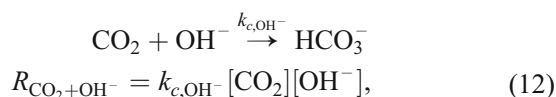
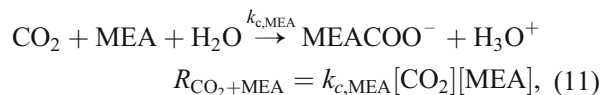
$$\ln K_{a,\text{MEA}^+} = -3.038 - \frac{7008.3}{T} - 0.0031T. \quad (8)$$

(v) Dissociation of carbamate [13]:



$$\ln K_{\text{carb}} = -0.52 - \frac{2545.5}{T}. \quad (10)$$

However, not all reactions reach equilibrium even though all are quite fast under the operating conditions of the system. In particular, for reactions involving carbon dioxide (Eq. (11) and Eq. (12)), kinetics (Eq. (13) and Eq. (14)) must be taken into account [14].



$$k_{c,\text{MEA}} = 4.32$$

$$\times 10^{13} \text{ m}^3 / (\text{kmol} \cdot \text{s}) \cdot \exp\left(\frac{-55.4603 \text{ kJ/mol}}{RT}\right), \quad (13)$$

$$k_{\text{OH}^-} = 9.77$$

$$\times 10^{10} \text{ m}^3 / (\text{kmol} \cdot \text{s}) \cdot \exp\left(\frac{-41.2564 \text{ kJ/mol}}{RT}\right). \quad (14)$$

Values of kinetic parameters are taken from Hikita et al. [16] for Eq. (11) and from Pinsent et al. [17] for Eq. (12).

3 Thermodynamic modeling

A good description of vapor-liquid equilibrium is crucial for a correct design of unit operations involving mass transfer from one phase to the other [18–25]. In particular, for a rate-based approach, in which mass transfer limitations are directly taken into account in the equations to be solved without resorting to the stage efficiency concept, a reliable prediction of the equilibrium composition is needed to correctly compute the driving force for the interphase mass transfer.

Acid gases and amines are weak electrolytes and partially dissociate in the aqueous phase to form a complex mixture containing molecular species and ionic species. Therefore the system is highly non-ideal in the liquid phase. The presence of ions and polar molecules creates significant thermal effects in solution. As for the gas phase, on the contrary, a negligible deviation from ideality has been observed, because of the low operating pressure which usually is atmospheric for the absorption but can be moderately higher when dealing with particular stripper configuration for MEA regeneration [6,14,18,26,27]. A γ/ϕ approach is often used: the behavior of the vapor phase is represented by means of an Equation of State, the SRK EoS [28], while the non-ideality of the liquid phase is reproduced using an activity coefficient model, the Electrolyte-NRTL model [29–32], where the excess Gibbs free energy is taken into account.

The model is characterized by a large number of parameters, which take into account interactions between molecule and molecule, molecule and ion pair, and ion pair and ion pair. It can be used to reproduce experimental data for a wide range of temperatures and loadings, if proper values of parameters are regressed. Vapor-liquid equilibrium experimental data for the system $\text{CO}_2\text{-H}_2\text{O-MEA}$ [33,34] have been collected in order to obtain calibrated parameters [14,27,35].

4 Mass transfer

4.1 Modeling with ASPEN Plus®

ASPEN Plus® is provided with a rate-based model, which takes into account the mass transfer limitations occurring in the absorption phenomenon. They are described with

film theory developed by Lewis and Whitman [36]. This theory assumes that all the mass transfer resistances are located into two films of a finite thickness close to the interface on the gas side and on the liquid side. These two films represent the controlling resistances to mass transfer from one phase to the other, since mixing by convection is so fast that the concentration of solute can be considered uniform for the bulk of the liquid or of the gas phases. A mass transfer coefficient can be derived, and it is proportional to the diffusivity of carbon dioxide in the aqueous phase, according to:

$$k_i^\circ = \frac{D_{\text{CO}_2}}{\delta}. \quad (15)$$

4.2 Proposed rate-based model

For amine scrubbing systems, the influence of diffusivity on the mass transfer coefficient is not as predicted by film theory [37]. Indeed, a square root dependence on diffusivity was observed and it can be correctly predicted [38] using the eddy diffusivity theory, proposed by King [12].

This theory assumes steady state conditions and takes into account both molecular diffusion and parallel turbulent transport, which, according to King, is “usually been accounted for through an eddy diffusivity”, by considering the presence of little eddies that influence the mass transfer rate. The eddy diffusivity is expressed as:

$$E = \varepsilon x^n + b, \quad (16)$$

where x is the distance from the interface along the semi-infinite coordinate and $n = 2$. At the interface ($x = 0$) there is no influence of eddies, so $b = 0$. Far from the interface, eddy diffusivity is the most important phenomenon. The boundary condition for $x \rightarrow \infty$ is $c = c_{\text{bulk}}$ [12].

Considering the contribute of eddy diffusivity to mass transfer and the presence of chemical reactions, the mass balance equation for carbon dioxide is:

$$\frac{\partial}{\partial x} \left[(D_{\text{CO}_2} + \varepsilon x^2) \frac{\partial [\text{CO}_2]}{\partial x} \right] - R_{\text{CO}_2} = 0, \quad (17)$$

where R_{CO_2} is the rate of consumption of carbon dioxide due to chemical reactions occurring in the liquid phase, D_{CO_2} the molecular diffusivity, and ε the parameter for eddy diffusivity of carbon dioxide in the solvent.

Since these reactions can be considered fast, with good approximation the interface pseudo first order (IPFO) assumption can be taken into account. Therefore, these reactions occur only in a small region close to the interface, the reaction sub-layer, which is a part of the boundary layer, and the concentrations of all species except CO_2 are assumed not to significantly change from their value at the interface. The extent of the reaction sub-layer depends on the kinetics involved. In the boundary layer region,

diffusion occurs, causing the liquid bulk concentration being different from that resulting in the reaction sub-layer.

Considering IPFO assumption and integrating Eq. (17), an expression for flux with a square root dependence on diffusivity, as required for a correct representation of the absorption phenomenon, is obtained:

$$N_{\text{CO}_2} = \frac{\pi}{2} \sqrt{\frac{1}{2}(k_{c,\text{OH}^-} [\text{OH}^-]_i + k_{c,\text{MEA}} [\text{MEA}]_i) D_{\text{CO}_2}} \times ([\text{CO}_2]_i - [\text{CO}_2]_{i,\text{eq}}), \quad (18)$$

where $[\text{CO}_2]_{i,\text{eq}}$ is the concentration of carbon dioxide in equilibrium with bulk composition. For a detailed description of the mathematical passages to obtain Eq. (18), see the Appendix.

The model previously described is properly introduced in ASPEN Plus[®] by linking an external Fortran subroutine, which is based on the eddy diffusivity theory, and it is successfully used for simulating an absorption column.

5 Results and discussion

The model is validated by simulating several test runs of an experimental pilot plant [39] with the aim to remove carbon dioxide from an exhaust gaseous stream coming from a coal-fired power plant with an aqueous solution of monoethanolamine (30% w/w).

Experimentally, 48 tests were run [39], 24 of them (from 1 to 24) with structured packing Flexypack 1Y and 24 of them (from 25 to 48) with random metal packing IMTP #40. However, according to the author [39], the first runs report trends that are inconsistent with the rest of the experimental campaign, so we focused on the cases involving the absorber with IMTP #40. Moreover, some of them, for example tests 45 and 46, are not taken into account, because the total material balance is not fulfilled, probably due to measurement inaccuracies of the instrumentation used or disturbances in the steady state operation [39]. For this reason, only the cases reported in

Tables 1 and 2 have been implemented.

The absorber is a packed column (packing type: IMTP #40, a random metal packing with a specific area of 145 m²/m³), composed of two beds, with a collector plate and a redistributor between them. It is characterized by an internal diameter of 42.7 cm and a total packing height of 6.10 m and is run at atmospheric pressure.

Results from simulations based on Eq. (18) have been compared with results from ASPEN Plus[®] default rate-based model and from the rate-based model referring to Eq. (19), proposed by Freguia and Rochelle [11] always on the basis of the eddy diffusivity theory.

$$N_{\text{CO}_2} = \sqrt{(k_{c,\text{OH}^-} [\text{OH}^-]_i + k_{c,\text{MEA}} [\text{MEA}]_i) \frac{D_{\text{CO}_2}}{\gamma_{\text{CO}_2}}} \times (a_{\text{CO}_2,i} - a_{\text{CO}_2,i}^*). \quad (19)$$

Freguia and Rochelle [11] in their model used a constant $k_{c,\text{MEA}}$ “adjusted to match commercial plant data” [11]. However, since no definite values of this constant have been found, the original value by Hikita et al. [40] has been considered for simulation. The multiplying factor $\sqrt{1/2} \pi/2$ of Eq. (19) has been obtained by analytically solving Eq. (17) and is not an adaptive parameter. Since Eq. (18) and Eq. (19) give rise to two different values of carbon dioxide flux, their application in modeling the MEA scrubbing process leads to different simulated performances of the absorption column.

The results of the simulated cases are shown in Table 1. As can be seen in Table 1, our model is able to predict a value of molar fraction of carbon dioxide in the purified gas coming out of the absorption column closer to the experimental value than by using ASPEN Plus[®] or Eq. (19).

For the simulated cases, the characteristics of the streams entering the absorber are shown in Table 2. Fig. 1 and Fig. 2 show the temperature profiles of two of the test run cases. In Figs. 1 and 2, a bulge is present because of the cold inlet gas absorbing heat from the rich solution.

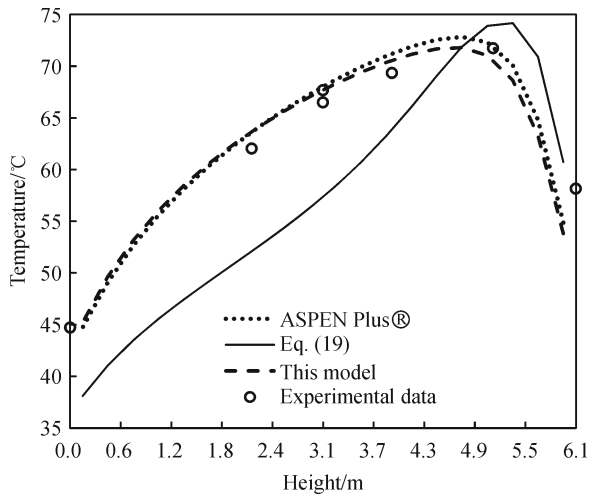
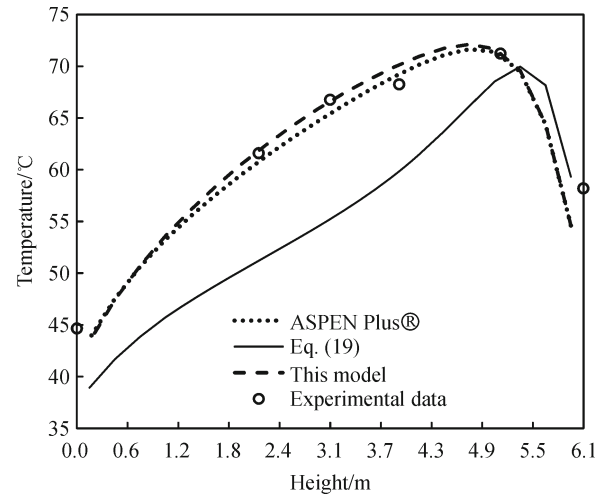
Table 1 CO₂ mole fraction in the purified gas

Test (Dugas, 2006)	Experimental data	ASPEN Plus [®] default		Eq. (19)		Our model	
	y_{CO_2} OUT	y_{CO_2} OUT	Absolute error/%	y_{CO_2} OUT	Absolute error/%	y_{CO_2} OUT	Absolute error/%
29	0.0532	0.04619	13.18	0.01704	67.97	0.05156	3.08
30	0.0591	0.05022	15.03	0.02381	59.71	0.05558	5.96
43	0.0558	0.04698	15.81	0.03328	40.36	0.05238	6.13
44	0.054	0.04655	13.80	0.03252	39.78	0.05203	3.65
47	0.0638	0.06682	4.73	0.06312	1.07	0.06753	5.85
48	0.0619	0.06339	2.41	0.05893	4.80	0.06374	2.97
		AAD %		AAD %		AAD %	
		10.82		35.61		4.61	

Table 2 Experimental data of the streams entering the absorption column for different cases

Case #	29		30		43	
Stream	gas IN	lean IN	gas IN	lean IN	gas IN	lean IN
T/K	324.14	313.15	324.69	313.15	326.66	313.15
P/atm	1.041	1.68	1.042	1.68	1.033	1.68
$F/(\text{kmol}\cdot\text{h}^{-1})$	25.8845	140.4958	25.7748	140.3816	25.4119	100.7471
Mole frac.						
H ₂ O	0.0164	0.8457	0.0163	0.8458	0.0163	0.8512
MEA	0	0.1201	0	0.1201	0	0.1209
CO ₂	0.1618	0.0342	0.1708	0.0341	0.1696	0.0279
O ₂	0.0484	0	0.0479	0	0.0479	0
N ₂	0.7734	0	0.7651	0	0.7662	0

Case #	44		47		48	
Stream	gas IN	lean IN	gas IN	lean IN	gas IN	lean IN
T/K	324.74	313.15	332.38	313.15	329.1	313.15
P/atm	1.033	1.68	1.02	1.68	1.016	1.68
$F/(\text{kmol}\cdot\text{h}^{-1})$	25.6271	101.1571	18.4596	77.3766	18.6061	77.0594
Mole frac.						
H ₂ O	0.0163	0.8512	0.0160	0.8461	0.0162	0.8457
MEA	0	0.1209	0	0.1202	0	0.1201
CO ₂	0.1680	0.0279	0.1841	0.0338	0.1763	0.0342
O ₂	0.0480	0	0.0471	0	0.0476	0
N ₂	0.7677	0	0.7528	0	0.7600	0

**Fig. 1** Experimental data [39] and temperature profile along the absorption column for the case # 44 reported in Table 2**Fig. 2** Experimental data [39] and temperature profile along the absorption column for the case # 47 reported in Table 2

Generally, the position of the bulge along the column depends on the value of the liquid to gas ratio [3]. Between the two packing beds in the pilot column a flow distributor is present: it helps in improving the column efficiency, but causes heat dissipations. For the sake of completeness, in Figs. 1 and 2 two different values of experimental

temperature are shown at a height of 3.1 m from the bottom, and were obtained by measuring the value above and below the distributor.

The temperature profiles obtained by ASPEN Plus® default and our model cross each other: for case # 44, this happens once, while for case # 47, this happens twice.

Since the amount of heat released during the process is proportional to the absorbed CO_2 , the same behavior can be observed also for the molar flow rate of CO_2 in the gas phase (Fig. 3 and Fig. 4).

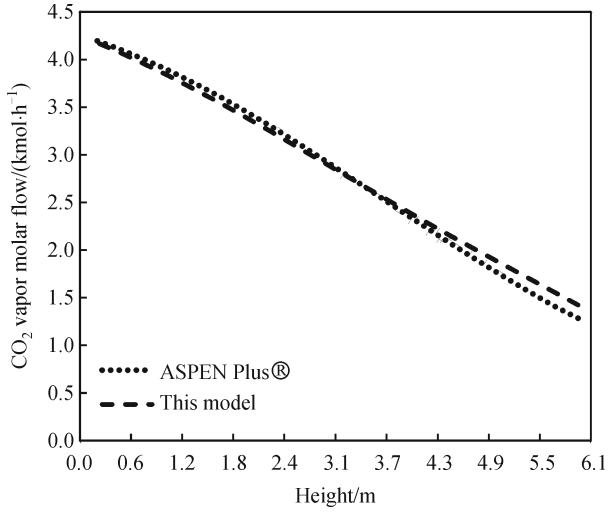


Fig. 3 Molar flow profile of carbon dioxide in the vapor phase along the absorption column for the case # 44 reported in Table 2

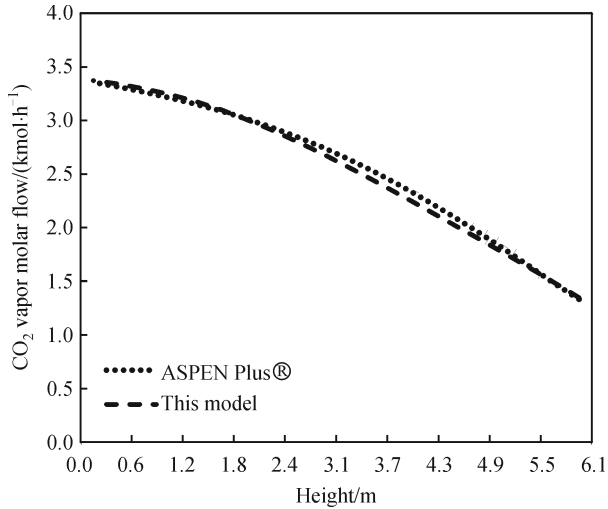


Fig. 4 Molar flow profile of carbon dioxide in the vapor phase along the absorption column for the case # 47 reported in Table 2

ASPEN Plus® well describes the temperature profile, but shows a per cent absolute average deviation of about 10.82% from experimental CO_2 molar fraction. Results obtained using Eq. (19) are far from experimental data, both for the estimation of carbon dioxide molar fraction (Table 1) and for the prediction of the temperature along the absorber. With our model the absorption tends to be slower, so that the concentration of carbon dioxide in the pure gas is close to experimental values. The position of the bulge is well predicted and deviations from experimental data are low (AAD% = 4.61%).

6 Conclusions

In this work a model is presented, where the eddy diffusivity theory [12] and the interfacial pseudo first order reaction assumption are taken into account. By comparison with experimental data of a pilot plant [39], the model shows a remarkable improvement in the prediction of the amount of carbon dioxide removed from the exhaust gas, with a good representation of the temperature profile, including the position of the bulge. The model may find application in acid gas absorption plants using amines, in order to design more accurate plants and to choose the right amount of solvent to be used.

Appendix

In the following the mathematical passages to obtain Eq. (18) starting from Eq. (17) are reported. A new kinetic constant ($k_{f,MEA_{cst}}$ and $k_{f,OH^-_{cst}}$), composed of the kinetic constant and the concentration of the other reactants assumed constant, can then be defined. Since, according to IPFO theory, the amine concentration is constant in the reaction sub-layer, also the concentration of products of amine is constant, it follows:

$$R_{\text{CO}_2} = k_{f,MEA_{cst}}([\text{CO}_2] - [\text{CO}_{2,eq}]_i),$$

where $[\text{CO}_{2,eq}]_i$ is the carbon dioxide concentration at equilibrium. Considering all the kinetically controlled reactions of the system the total rate of consumption of carbon dioxide is

$$R_{\text{CO}_2} = k_{f,\text{CO}_2}([\text{CO}_2] - [\text{CO}_{2,eq}]_i),$$

$$\text{with } k_{f,\text{CO}_2} = (k_{f,OH^-_{cst}} + k_{f,MEA_{cst}}).$$

Then

$$\frac{\partial^2 [\text{CO}_2]}{\partial r^2} - \frac{\pi^2}{4\epsilon} \left(1 + tg^2 \left(\frac{\pi r}{2}\right)\right) k_{f,\text{CO}_2} ([\text{CO}_2] - [\text{CO}_{2,eq}]_i) = 0,$$

$([\text{CO}_2] - [\text{CO}_{2,eq}]_i)$ and $-\frac{\pi^2}{4\epsilon} k_{f,\text{CO}_2}$ can be substituted, by obtaining:

$$\frac{\partial^2 y}{\partial r^2} + a \left(1 + tg^2 \left(\frac{\pi r}{2}\right)\right) y = 0.$$

This is a homogeneous linear differential equation with variable coefficients

$$a_0(r)y'' + a_1(r)y' + a_2(r)y = 0,$$

$$y = C_1 z(r) \int \frac{\exp \left(- \int \frac{a_1(r)}{a_0(r)} dr \right)}{z^2(r)} dr + C_2 z(r).$$

Since in this case $a_1(r) = 0$,

$$y = C_1 z(r) \int \frac{1}{z^2(r)} dr + C_2 z(r).$$

The following expression can be assumed for $z(r) \neq 0$,

$$z(r) = \alpha \left(\operatorname{tg} \left(\frac{\pi}{2} r \right) \right).$$

Then

$$\begin{aligned} & \alpha \frac{\pi^2}{2} \operatorname{tg} \left(\frac{\pi}{2} r \right) \left(1 + \operatorname{tg}^2 \left(\frac{\pi}{2} r \right) \right) \\ & + \alpha \left(1 + \operatorname{tg}^2 \left(\frac{\pi}{2} r \right) \right) \alpha \left(\operatorname{tg} \left(\frac{\pi}{2} r \right) \right) \\ & = 0, \end{aligned}$$

$$\operatorname{tg} \left(\frac{\pi}{2} r \right) \left(1 + \operatorname{tg}^2 \left(\frac{\pi}{2} r \right) \right) \left(\alpha \frac{\pi^2}{2} + a \cdot \alpha \right) = 0,$$

In order to satisfy the condition, it must be

$$\left(\alpha \frac{\pi^2}{2} + a \cdot \alpha \right) = 0.$$

This equation is satisfied for any value of α and when $a = -\pi^2/2$. A particular solution is identified, with α equal to 1,

$$z(r) = \operatorname{tg} \left(\frac{\pi}{2} r \right)$$

Then

$$y = C_1 \operatorname{tg} \left(\frac{\pi}{2} r \right) \int \frac{1}{\operatorname{tg}^2 \left(\frac{\pi}{2} r \right)} dr + C_2 \operatorname{tg} \left(\frac{\pi}{2} r \right),$$

$$y = -\frac{2}{\pi} C_1 \left(1 + \frac{\pi}{2} r \left(\operatorname{tg} \left(\frac{\pi}{2} r \right) \right) \right) + C_2 \operatorname{tg} \left(\frac{\pi}{2} r \right),$$

$$\begin{aligned} & [\text{CO}_2] - [\text{CO}_{2,\text{eq}}]_i \\ & = -\frac{2}{\pi} C_1 \left(1 + \frac{\pi}{2} r \left(\operatorname{tg} \left(\frac{\pi}{2} r \right) \right) \right) + C_2 \operatorname{tg} \left(\frac{\pi}{2} r \right). \end{aligned}$$

C_1 and C_2 can be evaluated considering the boundary conditions

$$[\text{CO}_2] = [\text{CO}_2]_i, \text{ when } x = 0,$$

and

$$[\text{CO}_2] = [\text{CO}_2]_i^*, \text{ when } x \rightarrow \infty.$$

Then the flux of carbon dioxide becomes

$$N_{\text{CO}_2} = \frac{\pi}{2} \sqrt{\varepsilon D_{\text{CO}_2}} ([\text{CO}_2]_i - [\text{CO}_{2,\text{eq}}]_i)$$

under condition that

$$a = -\frac{\pi^2}{2},$$

$$-\frac{k_{f,\text{CO}_2} \pi^2}{4\varepsilon} = -\frac{\pi^2}{2} \Rightarrow \varepsilon = \frac{k_{f,\text{CO}_2}}{2}.$$

The expression for the flux of carbon dioxide is

$$\begin{aligned} N_{\text{CO}_2} &= \frac{\pi}{2} \sqrt{\frac{1}{2} (k_{c,\text{OH}^-} [\text{OH}^-]_i + k_{c,\text{MEA}} [\text{MEA}]_i) D_{\text{CO}_2}} \\ &\quad \times ([\text{CO}_2]_i - [\text{CO}_2]_{i,\text{eq}}), \end{aligned}$$

with the correct dependence on diffusivity of carbon dioxide.

Nomenclature

[]	Concentration, kmol/m ³
a	Activity
D_{CO_2}	Diffusivity of carbon dioxide in the solvent, m ² /s
E	Eddy diffusivity, m ² /s
F	Molar flow, kmol/h
k	Kinetic constant, m ³ /(kmol·s)
k_i^o	Mass transfer coefficient of liquid film, m/s
K_{a,CO_2}	Equilibrium constant for the hydrolysis of dissolved carbon dioxide
K_{a,HCO_3^-}	Equilibrium constant for the dissociation of bicarbonate ion
$K_{a,\text{MEA}^{\text{H}^+}}$	Equilibrium constant for the dissociation of protonated MEA
K_{carb}	Equilibrium constant for the dissociation of carbamate
$K_{\text{H}_2\text{O}}$	Equilibrium constant for the dissociation of water
N_{CO_2}	Flux of carbon dioxide, kmol/(m ² ·s)
P	Pressure, bar
R	Rate of reaction, kmol/(m ³ ·s), or universal gas constant in Eq. (13) and in Eq. (14)
T	Temperature, K
x	Distance from the interface

Greek letters

ε	ε coefficient for Eddy diffusivity
γ_{CO_2}	Activity coefficient of carbon dioxide
δ	δ film thickness, m

Superscripts

*	Equilibrium
---	-------------

Subscripts

c	Kinetic
eq	Equilibrium
i	Interfacial

References

1. NOAA. 2013. <http://researchmatters.noaa.gov/news/Pages/Carbon-DioxideatMaunaLoareaches400ppm.aspx> (last accessed on May 15th, 2013)
2. UNO. Kyoto Protocol to the United Nations Framework Convention on Climate Change, 1998
3. Kohl A L, Nielsen R. Gas Purification, 5th ed. Texas: Gulf Publishing Company, Book Division, 1997
4. Wang M, Lawal A, Stephenson P, Sidders J, Ramshaw C. Post-combustion CO₂ capture with chemical absorption: A state-of-the-art review. *Chemical Engineering Research & Design*, 2011, 89(9): 1609–1624
5. Bergman D F, Yarborough L. In: 71st Annual Meeting of AIChE, Miami Beach, Florida, 1978
6. Moioli S, Pellegrini L A. Regeneration section of CO₂ capture plant by MEA scrubbing with a rate-based model. *Chemical Engineering Transactions*, 2013, 32: 1849–1854
7. Kent R L, Eisenberg B. Better data for amine treating. *Hydrocarbon Processing*, 1976, 55: 87–90
8. Al-Baghli N A, Pruess S A, Yesavage V F, Selim M S. A rate-based model for the design of gas absorbers for the removal of CO₂ and H₂S using aqueous solutions of MEA and DEA. *Fluid Phase Equilibria*, 2001, 185(1–2): 31–43
9. Mangalapally H P, Notz R, Hoch S, Asprien N, Sieder G, Garcia H, Hasse H. Pilot plant experimental studies of post combustion CO₂ capture by reactive absorption with MEA and new solvents. *Energy Procedia*, 2009, 1(1): 963–970
10. Kucka L, Müller I, Kenig E Y, Górak A. On the modelling and simulation of sour gas absorption by aqueous amine solutions. *Chemical Engineering Science*, 2003, 58(16): 3571–3578
11. Freguia S, Rochelle G T. Modeling of CO₂ capture by aqueous monoethanolamine. *AIChE Journal*. American Institute of Chemical Engineers, 2003, 49(7): 1676–1686
12. King C J. Turbulent liquid phase mass transfer at a free gas-liquid interface. *Industrial & Engineering Chemistry Fundamentals*, 1966, 5(1): 1–8
13. AspenTech. ASPEN Plus[®], Burlington, MA: AspenTech, 2010
14. Pellegrini L A, Moioli S, Gamba S. Energy saving in a CO₂ capture plant by MEA scrubbing. *Chemical Engineering Research & Design*, 2011, 89(9 9A): 1676–1683
15. Edwards T J, Maurer G, Newman J, Prausnitz J M. Vapor-liquid equilibria in multicomponent aqueous solutions of volatile weak electrolytes. *AIChE Journal*. American Institute of Chemical Engineers, 1978, 24(6): 966–976
16. Hikita H, Asai S, Ishikawa H, Honda M. The kinetics of reactions of carbon dioxide with monoethanolamine, diethanolamine and triethanolamine by a rapid mixing method. *Chemical Engineering Journal*, 1977, 13(1): 7–12
17. Pinsent B R W, Pearson L, Roughton F W J. The kinetics of combination of carbon dioxide with hydroxide ions. *Transactions of the Faraday Society*, 1956, 52: 1512–1518
18. Pellegrini L A, Moioli S, Picutti B, Vergani P, Gamba S. Design of an acidic natural gas purification plant by means of a process simulator. *Chemical Engineering Transactions*, 2011, 24: 271–276
19. Pellegrini L A, Moioli S, Gamba S, Ceragioli P. Prediction of vapor-liquid equilibrium for reservoir mixtures with cubic equations of state: binary interaction parameters for acidic gases. *Fluid Phase Equilibria*, 2012, 326: 45–49
20. De Guido G, Langè S, Moioli S, Pellegrini L A. Thermodynamic method for the prediction of solid CO₂ formation from multicomponent mixtures. *Process Safety and Environmental Protection*, 2014, 92(1): 70–79
21. Pellegrini L A, Langè S, Moioli S, Picutti B, Vergani P. Influence of gas impurities on thermodynamics of amine solutions. 1. Aromatics. *Industrial & Engineering Chemistry Research*, 2013, 52(5): 2018–2024
22. Langè S, Pellegrini L A, Moioli S, Picutti B, Vergani P. Influence of gas impurities on thermodynamics of amine solutions. 2. Mercaptans. *Industrial & Engineering Chemistry Research*, 2013, 52(5): 2025–2031
23. Gamba S, Soave G S, Pellegrini L A. Use of normal boiling point correlations for predicting critical parameters of paraffins for vapour-liquid equilibrium calculations with the SRK equation of state. *Fluid Phase Equilibria*, 2009, 276(2): 133–141
24. Pellegrini L A, Gamba S, Bonomi S, Calemma V. Equilibrium constants for isomerization of n-paraffins. *Industrial & Engineering Chemistry Research*, 2007, 46(16): 5446–5452
25. Pellegrini L A, Gamba S, Moioli S. Using an adaptive parameter method for process simulation of nonideal systems. *Industrial & Engineering Chemistry Research*, 2010, 49(10): 4923–4932
26. Oyekan B A, Rochelle G T. Energy performance of stripper configurations for CO₂ capture by aqueous amines. *Industrial & Engineering Chemistry Research*, 2005, 45(8): 2457–2464
27. Moioli S, Pellegrini L A, Gamba S. Simulation of CO₂ capture by MEA scrubbing with a rate-based model. In: 20th International Congress of Chemical and Process Engineering CHISA 2012, Prague, Czech Republic, 2012
28. Soave G. Equilibrium constants from a modified Redlich-Kwong equation of state. *Chemical Engineering Science*, 1972, 27(6): 1197–1203
29. Chen C C, Britt H I, Boston J F, Evans L B. Extension and application of the Pitzer equation for vapor-liquid equilibrium of aqueous electrolyte systems with molecular solutes. *AIChE Journal*. American Institute of Chemical Engineers, 1979, 25(5): 820–831
30. Chen C C, Britt H I, Boston J F, Evans L B. Local composition model for excess Gibbs energy of electrolyte systems. Part I: Single solvent, single completely dissociated electrolyte systems. *AIChE Journal*. American Institute of Chemical Engineers, 1982, 28(4): 588–596
31. Chen C C, Evans L B. A local composition model for the excess Gibbs energy of aqueous electrolyte systems. *AIChE Journal*.

- American Institute of Chemical Engineers, 1986, 32(3): 444–454
32. Mock B, Evans L B, Chen C C. Thermodynamic representation of phase equilibria of mixed-solvent electrolyte systems. *AIChE Journal*. American Institute of Chemical Engineers, 1986, 32(10): 1655–1664
 33. Jou F Y, Mather A E, Otto F D. The Solubility of CO₂ in a 30-mass-percent monoethanolamine solution. *Canadian Journal of Chemical Engineering*, 1995, 73(1): 140–147
 34. Ma'mun S, Nilsen R, Svendsen H F, Juliussen O. Solubility of carbon dioxide in 30 mass % monoethanolamine and 50 mass % methyldiethanolamine solutions. *Journal of Chemical & Engineering Data*, 2005, 50(2): 630–634
 35. Gamba S, Pellegrini L A. Biogas upgrading: Analysis and comparison between water and chemical scrubbing. *Chemical Engineering Transactions*, 2013, 32: 1273–1278
 36. Lewis W K, Whitman W G. Principles of gas absorption. *Industrial & Engineering Chemistry*, 1924, 16(12): 1215–1220
 37. Moioli S, Pellegrini L A, Picutti B, Vergani P. Improved rate-based modeling of H₂S and CO₂ removal by MDEA scrubbing. *Industrial & Engineering Chemistry Research*, 2013, 52(5): 2056–2065
 38. Austgen D M A. Model of vapor-liquid equilibria for acid gas-alkanolamine-H₂O systems. Dissertation for the Doctoral Degree. Texas: University of Texas, 1989
 39. Dugas R E. Pilot plant study of carbon dioxide capture by aqueous monoethanolamine. Dissertation for the Master Degree. Texas: The University of Texas, 2006
 40. TRC. Selected Values of Properties of Chemical Compounds. Texas: Texas A&M University, College Station, 1980